Dokkyo Journal of Medical Sciences
47(1) : 1 ～ 8, 2020

Original

What Affects the Visualization of Prostate Cancer Using MRI in Patients Treated with RARP?

Kensuke Inamura[a], Yasushi Kaji[a], Yosuke Misu[a], Mariko Kumazawa[a], Atsushi Suzuki[a], Masahiro Yashi[b], Takao Kamai[b]

[a]*Department of Radiology, Dokkyo Medical University, Mibu, Tochigi, Japan*
[b]*Department of Urology, Dokkyo Medical University, Mibu, Tochigi, Japan*

SUMMARY

Aim : To assess the index lesions (the largest and clinically significant ones) in cases of surgically confirmed prostate cancer (PCa) using a multi-parametric MRI at 3 tesla and to evaluate the relationships between the clinical-pathological features of index PCas and cancer visualization.

Materials and Methods : This retrospective study included 67 patients who had undergone robotic-assisted radical prostatectomy. Two radiologists reviewed the MRIs (axial and coronal T2-weighted imaging, diffusion-weighted imaging (DWI) with apparent diffusion coefficient mapping and dynamic contrast enhancement MRI (DCEI)). The patients were divided into 4 groups as follows : detected on all 3 sequences (A), on 2 of 3 sequences (B), on 1 of 3 sequences (C), and on none of them (D). In all groups, all PCa characteristics were assessed, including the PSA level, Grade Group (GG) based on the Gleason score (GS), the D'Amico criteria, and the maximum tumour length (TL) of the biopsy specimen.

Results : Of the 67 patients, 16 were high-risk according to the D'Amico criteria, and 15 of these 16 high-risk patients (94%) belonged to either Group A or Group B. In addition, the mean TL and GG were longer and higher, respectively, in Group A than in the other groups ($p<0.05$). Furthermore, in Group B, 3 of the 4 high-risk patients (75%) were detected using DWI and DCEI. The lesions detected using DWI and DCEI had higher GSs and were in a higher GG.

Conclusion : PCas of pathologically higher grades and clinically higher risk were more readily detectable using multiple parameters.

Key Words : Prostate cancer, multi-parametric MRI, dynamic contrast enhancement MRI, diffusion-weighted imaging

INTRODUCTION

It has been estimated that the number of new prostate cancer (PCa) cases yearly is 164,690, and PCa is the second most common cause of cancer-related mortality for males in the United States. In Japan, 78,400 new PCa cases are estimated yearly, and it is the sixth leading cause of cancer deaths[1,2].

Currently, the primary diagnostic approaches for PCa are the serum prostate-specific antigen (PSA)

Received October 4, 2019 ; accepted November 8, 2019
Reprint requests to : Kensuke Inamura
Department of Radiology, Dokkyo Medical University, 880 Kitakobayashi, Mibu-machi, Shimotsuga-gun, Tochigi, 321-0293 Japan.

test and/or an abnormal digital rectal examination (DRE). The standard PCa diagnostic pathway is biopsy guided by transrectal ultrasound (TRUS) and using multiple needles to systematically sample the entire prostate gland without knowledge of the likely locations of tumours.

Because of developments in magnetic resonance imaging (MRI), including diffusion-weighted imaging (DWI), prostate MRI has become a common mode of detecting PCa. The PCa detection rate is particularly improved using the multi-parametric MRI (mp-MRI) approach, which combines several imaging sequences, including T2-weighted imaging (T2WI), DWI, dynamic contrast enhancement MRI (DCEI), and, less commonly, MR spectroscopy. T2WI is the backbone of prostate imaging and provides both anatomical and structural information. DWI and DCEI are functional approaches, with the former reflecting the diffusibility of the water molecules in the intra- and extra-cellular spaces, and DCEI representing the vascularity in the PCa.

Although mp-MRI cannot depict all prostate lesions, in prostatectomy histologic correlation studies, mp-MRI findings have shown that a tumour's visibility and detectability depend on its size, volume[3~6] and Gleason score (GS)[3,5,6]. Some studies have found that tumours larger than 1.0 cm or 0.5 cc and having a GS greater than or equal to 7 were detectable. However, these studies used a combination of approaches (T2WI, DWI and DCEI). In the Prostate Imaging Reporting and Data System (PI-RADS) version 2[7], which is a relatively new way of using mp-MRI to detect PCas, the contribution of DCEI has been defined as secondary to those of T2WI and DWI because DCEI's additional value has not been firmly established. Nevertheless, DCEI is often helpful in detecting PCas in actual clinical readings.

The purpose of the present study was to use mp-MRI at 3T to assess index lesions, which are the largest and most clinically significant ones, in cases of surgically confirmed PCa and to evaluate the relationships between the clinical-pathological features of index lesions and cancer visualization.

MATERIALS AND METHODS

Patients

The Independent Ethics Committee of our hospital approved this retrospective study without the need for specific patient consent. The study included 151 consecutive patients who had clinically significant cancer, which was defined as having a GS≥7 and/or a volume≥0.5 cc and/or an extra-prostatic extension, and who had undergone robotic-assisted radical prostatectomy (RARP) between October 2012 and December 2014. The study' exclusion criteria included prior hormonal or radiation treatment, lack of history of a prostate 3 tesla (3T) MRI in the year before the RARP and lack of a DCEI. The patients' ages ranged from 55 to 76 years (median age 66 years), with serum PSA values ranging from 3.7 to 30.7 ng/mL (median 5.8 ng/mL).

MR imaging Technique

The subjects were scanned using a 3T MR scanner (Magnetom Trio Tim, Siemens Medical Solutions ; Erlangen, Germany) and a combination of a spine matrix coil (32 ch) and a body matrix coil (18 ch). No endorectal coil was used. The patients had not been given laxatives and had not received an intramuscular injection of butyl scopolamine or glucagon before MR examination.

Axial T2WIs (repetition time (TR)/echo time (TE) =5000/93 ms) were obtained using a 3-mm thickness, a 1-mm interslice gap, a 200×200 mm field of view (FOV) and a 320×320 matrix. The voxel size was 0.625×0.625×3.0 mm, equalling a volume of 1.17 mm^3. The echo train length was 13.

DWIs were obtained, and an apparent diffusion coefficient (ADC) mapping was calculated for each slice. Axial DWIs were obtained using a Stejskal-Tanner spin-echo echo-planar imaging sequence that had the following parameters : TR-TE of 6000/78 ms, flip angle of 90° , NEX of 6, b values of 0, 1000 and 1500 s/mm^2, matrix of 128×92, FOV of 350×250 mm, a slice thickness/gap of 3/1 mm to cover the entire prostate and a generalized autocalibrating partially parallel acquisition (GRAPPA) algorithm. The GRAPPA's parameters were set to acceleration factors of 2. The voxel size was 2.734×2.734×3.0 mm, equalling a

Table 1 Cancer detection criteria

T2WI for PZ	
4	Discrete, homogeneous low-signal focus/mass confined to the prostate
5	Discrete, homogeneous low-SI focus with extracapsular extension/invasive behavior of mass effect on the capsule (bulging), or broad (>1.5 cm) contact with the surface
T2WI for TZ	
4	Areas of more homogeneous low SI, ill defined : "erased charcoal sign"
5	Same as category 4. but involving the anterior fibromuscular stroma or the anterior horn of the PZ. Usually lenticular or water-drop shaped
DWI	
4	Focal areas of reduced ADC but isointense SI on high-b-value images (b≥800 sec/min[2])
5	Focal area/mass of hyper SI on high-b-value image (b≥800 sec/min[2]) with reduced ADC
DCEI	
4	For focal enhancing lesion with curve type 2-3 (plateau or washout pattern)
5	For asymmetric lesion of lesion at an unusual place with curve type 2-3

T2WI, T2-wighted imaging ; DWI, diffusion-weighted imaging, DCEI, dynamic contrast enhancement magnetic resonance imaging ; PZ, peripheral zone ; TZ, transition zone ; SI, signal intensity ; ADC, apparent diffusion coefficient.

volume of 22.3 mm^3. The imaging location of the DWIs was identical to that of the T2WIs.

A gadolinium-DCEI during volumetric interpolated breath-hold examination was performed for a total acquisition time of 20 s in the axial orientation using a TR/TE of 3.5/1.3 ms, a matrix of 256×236, an FOV of 300×300 mm and a slice thickness/gap of 3/0 mm. The voxel size was 1.17×1.27×3.0 mm, equalling 4.47 mm^3. For this dynamic scanning procedure, pre-contrast baselines were sequentially obtained 50, 70 and 90 s after bolus injection of 0.1 mmol/kg of gadopentetate dimeglumine (Magnevist, Bayer Schering Pharma ; Berlin, Germany), followed by a 15-mL saline flush-out at a rate of 3.0 mL/s. A 240-s delayed -phase series was added as a T1-weighted spin-echo image.

Image Interpretation

The MR images of the PCa patients were retrospectively reviewed by two radiologists (one with 20 years' experience in reading prostate MRIs and the other with 5 years' experience) who had no knowledge of either the histopathologic findings or the clinical data. When interpretations differed, the findings of the radiologist with 20 years' experience were deferred to.

Although PI-RADS version 2[7] had already been released, PI-RADS version 1[8] was used to determine whether cancer was depicted on the MRI. This was because in PI-RADS version 2, a DCEI can be assessed using only two scores (+and−), while in PI-RADS version 1, a DCEI can be assessed using an enhancement curve. Besides a $score_{t2wi}$ 4-5 and a $score_{dwi}$ 4-5 in PI-RADS version 1, we determined that both 'for focal enhancing lesion with curve type 2-3 (plateau or washout pattern)' and 'asymmetric lesion or lesion at an unusual place with cure type 2-3' were a $score_{dcei}$ 4-5. In each sequence, score 4-5 was positive for cancer on the MRI (Table 1). In cases of more than one cancerous region, the study targeted the largest lesion as determined using the histopathological findings from the prostatectomy.

Data and Statistical Analysis

The cases were divided into following four groups : those detected on all three sequences (Group A ; Figure 1), on two of the three sequences (Group B ; Figure 2), on one of the three sequences (Group C) and

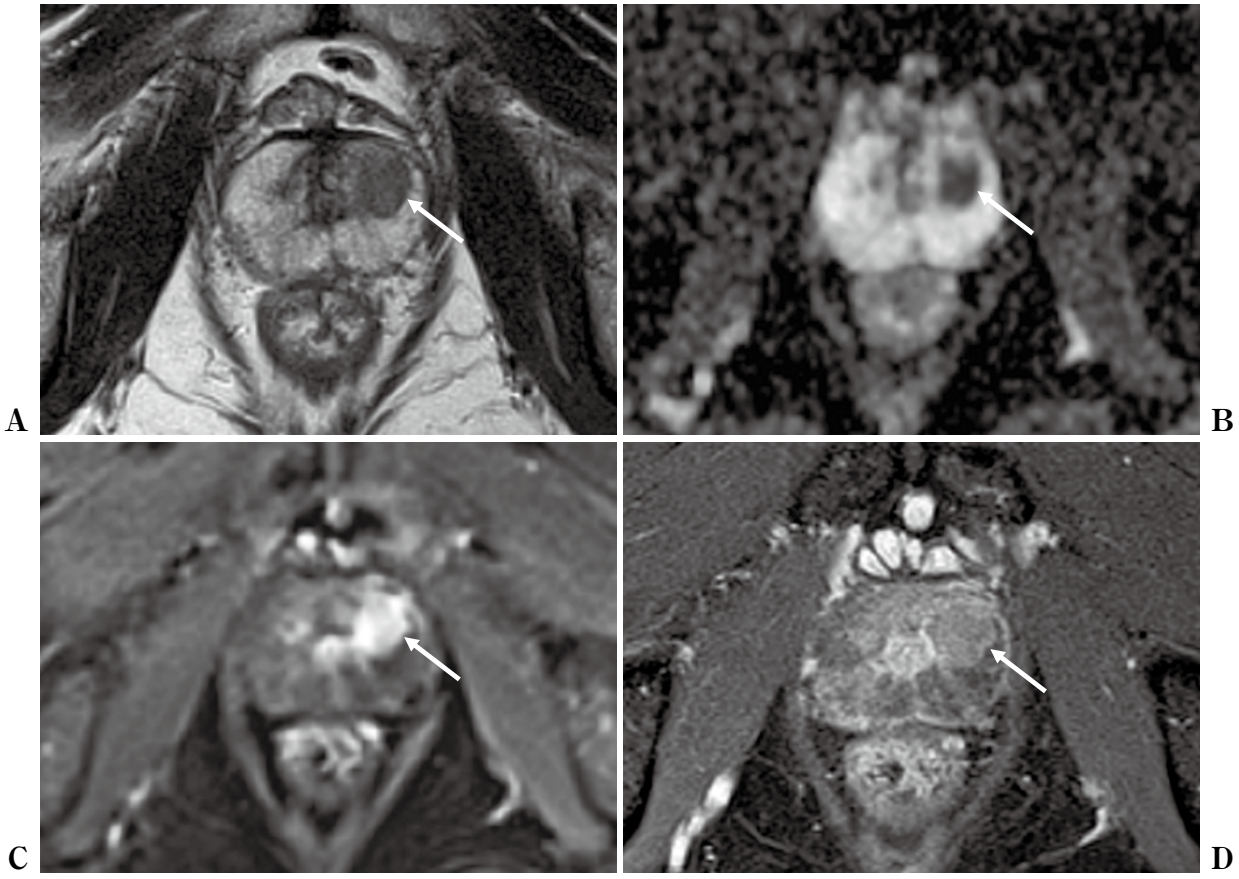

Figure 1

Multi-parametric MRI for a 75-year-old male with high risk prostate cancer (biopsy Gleason score 4+4, robotic-assisted radical prostatectomy Gleason score 4+5, prostate-specific antigen 5.2 ng/mL). (**A**) T2-weighted imaging showed homogeneous hypo-intensity mass in the left peripheral zone ($score_{t2wi}$ 4). (**B**) the mass had reduced apparent diffusion coefficient ($score_{dwi}$ 5). (**C, D**) dynamic contrast enhancement MR imaging showed asymmetric washout pattern ($score_{dcei}$ 5). This case was assigned to Group-A.

on none of them (Group D). Based on previous studies[9~12], the following PCa characteristics were assessed : PSA level, Grade Group (GG) based on GS[13], maximum tumour length (TL) of the biopsy specimen and D'Amico criteria[14]. D'Amico criteria are some of the most widely used for assessing PCa risk and are designed to evaluate the risk of recurrence following localized treatment of PCa. The GGs and GSs of both the biopsy specimen and the prostatectomy were evaluated. All parameters were statistically analysed using the Steel-Dwass test with R (version 3.3.2) to enable multiple comparisons. A $p \leq 0.05$ was regarded as statistically significant.

RESULTS

All 67 patients (mean age 66.0 years, median PSA 5.91 ng/mL) met the study's inclusion criteria. Table 2 shows the PCa characteristics of each group in the study. 3T MRI with any sequence (T2WI, DWI or DCEI, respectively) could detect PCa with a higher sensitivity (83.6% ; 56/67) than could T2WI (55.2% ; 37/67), DWI (64.2% ; 43/67) and DCEI (64.2% ; 43/67) (Table 2).

Of the 67 patients, 29 were assigned to Group A, 13 to Group B, 14 to Group C and 11 to Group D (Table 3). In addition, 16 of the 67 patients were high-risk according to the D'Amico criteria, and 15 of those 16 (94%) belonged to either Group A or B. The other high-risk patient belonged to Group D. There were statistically significant differences in the D'Amico criteria between Groups A and C ($p=0.005$) and between Groups A and D ($p=0.0072$). Furthermore,

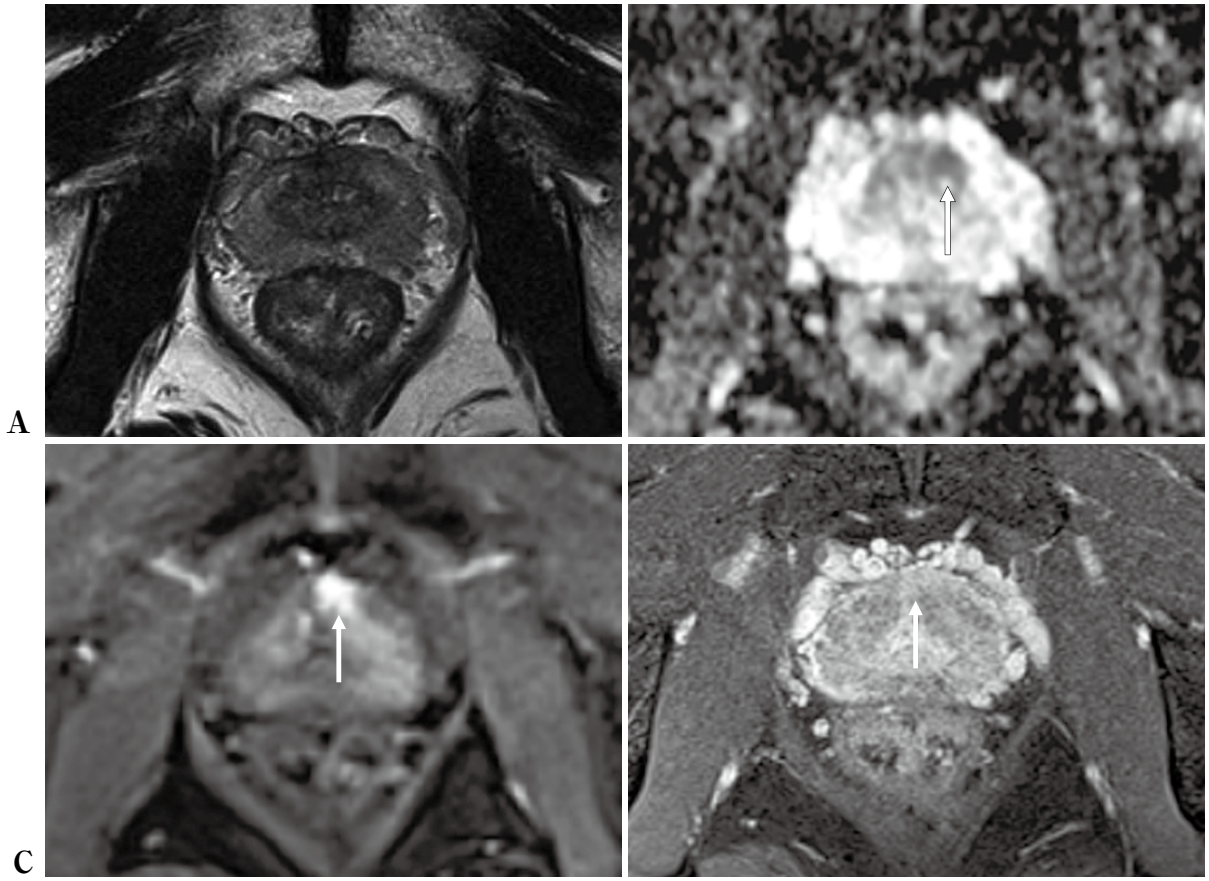

Figure 2

Multi-parametric MRI for a 69-year-old male with high risk prostate cancer (biopsy Gleason score 4+4, robotic-assisted radical prostatectomy Gleason score 4+3, prostate-specific antigen 10.0ng/mL). (**A**) T2-weighted imaging could not depict hypo-intensity mass clearly due to diffuse mild hypo-intensity in the peripheral zone ($score_{t2wi}$ 3). (**B**) the mass had reduced apparent diffusion coefficient ($score_{dwi}$ 5). (**C, D**) dynamic contrast enhancement MR imaging showed asymmetric plateau pattern ($score_{dcei}$ 5). This case was assigned to Group-B.

Table 2 Patient characteristics classified by cancer-detected sequences

cancer-detected sequences (N)	median PSA (ng/mL)	average TL (mm)	D'Amico criteria	average GG Bx	average GS Bx	average GG RARP	average GS RARP
T2WI (37)	6.4	6.7	L6/Int 18/H13	2.6	7.1	2.9	7.3
DWI (43)	5.9	6.2	L6/Int 22/H 15	2.6	7.2	2.9	7.2
DCEI (43)	6.4	6.0	L5/Int 23/H15	2.7	7.2	2.9	7.3
any (56)	6.2	5.7	L10/Int 31/H 15	2.5	7.1	2.8	7.2

N, Number of patients ; T2WI, T2-wighted imaging ; DWI, diffusion-weighted imaging, DCEI, dynamic contrast enhancement magnetic resonance imaging ; PSA, prostate-specific antigen ; TL, maximum tumor length of the biopsy specimen ; GG, Gleason grade group system based on Gleason scoring system ; GS, Gleason scoring system, Bx, biopsy specimen ; RARP, robotic-assisted radical prostatectomy ; L, low risk ; Int, intermediate risk ; H, high risk.

Table 3 Patient characteristics classified by group A–D (number of detected sequences)

group (N)	median PSA (ng/mL)	average TL (mm)	D'Amico criteria	average GG Bx	average GS Bx	average GG RARP	average GS RARP
A (29)	6.4	6.7	L1/Int 17/H 11	2.8	7.3	3.1	7.4
B (13)	6.4	6.2	L5/Int 4/H 4	2.4	7.0	2.4	7.0
C (14)	5.8	3.0	L4/Int 10/H 0	1.8	6.7	2.4	6.9
D (11)	5.6	3.8	L6/Int 4/H 1	1.7	6.4	2.4	7.2

N, Number of patients ; PSA, prostate-specific antigen ; TL, maximum tumor length of the biopsy specimen ; GG, Gleason grade group system based on Gleason scoring system ; GS, Gleason scoring system, Bx, biopsy specimen ; RARP, robotic-assisted radical prostatectomy ; L, low risk ; Int, intermediate risk ; H, high risk.

Table 4 Patient characteristics classified in group B

subgroup (N)	positive sequences	median PSA (ng/mL)	average TL (mm)	D'Amico criteria	average GG Bx	average GS Bx	average GG RARP	average GS RARP
B1 (4)	DWI + DCEI	6.2	6.5	L0/Int 1/H3	3.8	8.0	2.5	7
B2 (6)	T2 + DWI	7.7	5.3	L4/Int 1/H1	1.7	6.5	2	6.7
B2 (3)	T2 + DCEI	10.3	7.7	L1 / Int 2 / H0	2.0	6.7	3	7.7

N, Number of patients ; PSA, prostate-specific antigen ; TL, maximum tumor length of the biopsy specimen ; GG, Gleason grade group system based on Gleason scoring system ; GS, Gleason scoring system, Bx, biopsy specimen ; RARP, robotic-assisted radical prostatectomy ; L, low risk ; Int, intermediate risk ; H, high risk.

in the mean TL of the biopsy specimens, there were statistically significant differences between Groups A and C ($p=0.002$) and between Groups B and C ($p=0.028$). There were also statistically significant differences in the GGs of the biopsies between Groups A and C ($p=0.020$) and Groups A and D ($p=0.034$). There were statistically significant differences in the average GSs of the biopsies between Groups A and C ($p=0.043$) and Groups A and D ($p=0.028$). In the GGs of the RARP cases, although the differences were not statistically significant, differences were observed between Groups A and B ($p=0.067$), Groups A and C ($p=0.072$) and Groups A and D ($p=0.064$).

3T MRI (used in groups A–C) had a 93.8% (15/16) sensitivity in detecting index lesions in the high-risk patients. In Group B, the index lesions in 3 of the 4 high-risk patients (75%) were detected using DWI and DCEI (Table 4), and those lesions tended to have higher GSs ($p=0.073$) and higher GGs ($p=0.086$), according to their biopsy results.

DISCUSSION

The results of the present study showed that the PCas detected on all three sequences were pathologically higher grade and clinically higher risk. In addition, the PCas detected on more than two sequences had a relationship with the TL of the biopsy specimen. Yoshida et al.[10] found that TL was strongly significantly associated with PCas that could be detected using 3T MRI, and that result corresponds with those of the present study.

In the present study's series, the sensitivities in detecting PCa were 83.6% (56/67) for mp-MRI, 56.7 % (38/67) for T2WI alone, 67.2% (45/67) for DWI alone and 65.7% (44/67) with DCEI alone. DWI was not shown to be superior to DCEI.

Although few studies have found a correlation between GS and DCEI, DCEI represents the microvascular properties and angiogenesis using intravenous gadolinium contrast. Lovegrove et al.[15] found that malignant prostate lesions had increased tumour vascularity and early and rapid enhancement, followed by a rapid washout of the contrast administered. DWI represents the random Brownian motion of water molecules. Because PCa causes increased cellularity and decreased extracellular spaces, it theoretically

results in restricted diffusion. Some studies have noted that DWI may help to differentiate between low-risk and high-risk PCas[11,16,17]. Costa et al.[17] reported that clinically significant PCas had lower mean ADC values than those with clinically insignificant lesions (overall, 0.598 vs. 0.803 $mm/s^2 \times 10^{-3}$; PZ, 0.597 vs. 0.855 $mm/s^2 \times 10^{-3}$; TZ, 0.600 vs. 0.660 $mm/s^2 \times 10^{-3}$). Because a PCa that has a lower ADC value is more readily detectable using the ADC map, we evaluated the ADC map visually and saw a similar trend in the present study, although we did not measure ADC values.

In the present study, even in the group that was high-risk according to the D'Amico criteria, only 1 of 67 (1.4%) PCas could not be detected on any of the three sequences. In this case, the MR images were degraded by peristalsis and rectal gas. Although prostate MRIs at 3T provide both a higher signal-to-noise ratio and high-quality images without the use of an endorectal coil, they are associated with a significant increase in imaging artefacts, including geometric distortion and signal graininess, especially DWIs[18]. Although the endorectal coil has some disadvantages, including patient discomfort, gland deformation and enema preparation, it is helpful not only for improving images but also for avoiding artefacts that result from rectal gas across the prostate.

Current mp-MRIs for PCa that are based on the PI-RADS version 2[7] scoring system have assessment categories for each lesion that are based on the scoring of T2WI, DWI and DCEI sequences with the dominant sequence, including T2WI for the transition zone and DWI for the peripheral zone. The present study found that the number of positive sequences in the three sequences (T2WI, DWI and DCEI) were related to the GS or the risk criteria. The approach to Category 3 (equivalent to clinically significant PCa) based on PI-RADS version 2 is still controversial[19,20], and the results of the present study could suggest a simplified approach to evaluating and managing Category 3 PCas.

The present study has some limitations, including its retrospective design, its single-centre site and some discrepancies in the GSs and GGs between the biopsy pathology and the RARP pathology. Discrepancies in the GSs of specimens obtained using needle biopsies versus radical prostatectomies are common and universal[21]. In the treatment algorithms, the highest GS is typically used as the overall one, even if a lower GS predominates. This practice has the potential to misrepresent the overall cancer in the entire gland for some patients and places them in a higher GG[22].

In conclusion, PCas that were detectable on more than two sequences using prostate mp-MRI were pathologically higher grade and clinically higher risk.

Conflict of interest

The authors declare no conflict of interest.

REFERENCES

1) American Cancer Society : Cancer facts and figures 2018. https://www.cancer.org/content/dam/cancer-org/research/cancer-facts-and-statistics/annual-cancer-facts-and-figures/2018/cancer-facts-and-figures-2018.pdf. Accessed November 12, 2018.
2) Center for Cancer Control and Information Services, National Cancer Center Japan : Projected Cancer Statistics, 2018. https://ganjoho.jp/en/public/statistics/short_pred.html. Accessed November 12, 2018.
3) Le JD, Tan N, Shkolyar E, et al : Multifocality and prostate cancer detection by multiparametric magnetic resonance imaging : correlation with whole-mount histopathology. Eur Urol **67** : 569-576, 2015.
4) Bratan F, Niaf E, Melodelima C, et al : Influence of imaging and histological factors on prostate cancer detection and localization on multiparametric MRI : a prospective study. Eur Radiol **23** : 2019-2029, 2013.
5) Turkbey B, Mani H, Shah V, et al : Multiparametric 3T prostate magnetic resonance imaging to detect cancer : histopathological correlation using prostatectomy specimens processed in customized magnetic resonance imaging based molds. J Urol **186** : 1818-1824, 2011.
6) Rosenkrantz AB, Mendrinos S, Babb JS, et al : Prostate cancer foci detected on multiparametric magnetic resonance imaging are histologically distinct from those not detected. J Urol **187** : 2032-2038, 2012.
7) Weinreb JC, Barentsz JO, Choyke PL, et al : PI-RADS Prostate Imaging-Reporting and Data Sys-

tem : 2015, Version 2. Eur Urol **69** : 16-40, 2016.
8) Barentsz JO, Richenberg J, Clements R, et al : ESUR prostate MR guidelines 2012. Eur Radiol **22** : 746-757, 2012.
9) Epstein JI, Egevad L, Amin MB, et al : The 2014 International Society of Urological Pathology (ISUP) Consensus Conference on Gleason Grading of Prostatic Carcinoma : Definition of Grading Patterns and Proposal for a New Grading System. Am J Surg Pathol **40** : 244-252, 2016.
10) Yoshida R, Kaji Y, Tamaki Y, et al : Information of prostate biopsy positive core : does it affect MR detection of prostate cancer on using 3T-MRI? Jpn J Radiol **33** : 246-252, 2015.
11) Woodfield CA, Tung GA, Grand DJ, et al : Diffusion-weighted MRI of peripheral zone prostate cancer : comparison of tumor apparent diffusion coefficient with Gleason score and percentage of tumor on core biopsy. AJR Am J Roentgenol **194** : W316-W322, 2010.
12) Rastinehad AR, Baccala AA Jr, Chung PH, et al : D'Amico risk stratification correlates with degree of suspicion of prostate cancer on multiparametric magnetic resonance imaging. J Urol **185** : 815-820, 2011.
13) Pierorazio PM, Walsh PC, Partin AW, et al : Prognostic Gleason grade grouping : data based on the modified Gleason scoring system. BJU Int **111** : 753-760, 2013.
14) D'Amico AV, Whittington R, Malkowicz SB, et al : Biochemical outcome after radical prostatectomy, external beam radiation therapy, or interstitial radiation therapy for clinically localized prostate cancer. JAMA **280** : 969-974, 1998.
15) Lovegrove CE, Matanhelia M, Randeva J, et al : Prostate imaging features that indicate benign or malignant pathology on biopsy. Transl Androl Urol **7** : S420-S435, 2018.
16) Hambrock T, Somford DM, Huisman HJ, et al : Relationship between apparent diffusion coefficients at 3.0-T MR imaging and Gleason grade in peripheral zone prostate cancer. Radiology **259** : 453-461, 2011.
17) Costa DN, Xi Y, Aziz M, et al : Prospective Inclusion of Apparent Diffusion Coefficients in Multiparametric Prostate MRI Structured Reports : Discrimination of Clinically Insignificant and Significant Cancers. AJR Am J Roentgenol **212** : 109-116, 2019.
18) Mazaheri Y, Vargas HA, Nyman G, et al : Image artifacts on prostate diffusion-weighted magnetic resonance imaging : trade-offs at 1.5 Tesla and 3.0 Tesla. Acad Radiol **20** : 1041-1047, 2013.
19) Scialpi M, Martorana E, Aisa MC, et al : Score 3 prostate lesions : a gray zone for PI-RADS v2. Turk J Urol **43** : 237-240, 2017.
20) Thai JN, Narayan HA, George AK, et al : Validation of PI-RADS Version 2 in Transition Zone Lesions for the Detection of Prostate Cancer. Radiology **288** : 485-491, 2018.
21) Khoddami M, Khademi Y, Kazemi Aghdam M, et al : Correlation between Gleason Scores in Needle Biopsy and Corresponding Radical Prostatectomy Specimens : A Twelve-Year Review. Iran J Pathol **11** : 120-126, 2016.
22) Arias-Stella JA 3rd, Shah AB, Montoya-Cerrillo D, et al : Prostate biopsy and radical prostatectomy Gleason score correlation in heterogenous tumors : proposal for a composite Gleason score. Am J Surg Pathol **39** : 1213-1218, 2015.